Temporal Evolution of the Size Distribution during Exchange Kinetics of Pluronic P103 at Low Temperatures

ARTICLE *in* THE JOURNAL OF PHYSICAL CHEMISTRY B · APRIL 2009

Impact Factor: 3.3 · DOI: 10.1021/jp809685q · Source: PubMed

4 AUTHORS, INCLUDING:

J. F. A. Soltero
University of Guadalajara
64 PUBLICATIONS **951** CITATIONS
SEE PROFILE

Jorge E. Puig
University of Guadalajara
193 PUBLICATIONS **2,889** CITATIONS
SEE PROFILE

Yahya Rharbi
French National Centre for Scientific Resea…
60 PUBLICATIONS **1,092** CITATIONS
SEE PROFILE

THE JOURNAL OF PHYSICAL CHEMISTRY B

Article

Temporal Evolution of the Size Distribution during Exchange Kinetics of Pluronic P103 at Low Temperatures

V. V. A. Fernandez, J. F. A. Soltero, J. E. Puig, and Y. Rharbi

J. Phys. Chem. B, **Article ASAP** • Publication Date (Web): 18 February 2009

Temporal Evolution of the Size Distribution during Exchange Kinetics of Pluronic P103 at Low Temperatures

V. V. A. Fernandez,[†,‡] J. F. A. Soltero,[†,‡] J. E. Puig,[‡] and Y. Rharbi*[,†]

Laboratoire de Rhéologie, UJF/INPG/CNRS, UMR 5520, B.P.53, F-38041 Grenoble Cedex 9, France, and Departamentos de Ingeniería Química, Universidad de Guadalajara, Boul. M. García Barragán # 1451, Guadalajara, Jal. 44430, México

Received: November 2, 2008; Revised Manuscript Received: January 1, 2009

The micellar dynamics of many (PEO-PPO-PEO) triblock copolymers have been extensively investigated throughout the past decade using ultrasonic relaxation or temperature jump experiments. These methods primarily use the total scattering intensity to quantify the exchange mechanisms, and these results are then interpreted to get an idea about temporal evolution of the micelle size and size distribution. In this paper, we present experiments where we directly measure the size of the micelles and the size distribution during the exchange kinetic of the pluronic triblock copolymer P103. Solutions of the commercial P103 surfactant form premicelle aggregates in the proximity of the critical micelle temperature and proper micelles at high temperatures. The kinetics of evolution from aggregates to proper micelles is investigated using dynamic light scattering after a temperature jump. The temporal evolution of the scattering intensity and the average size as well as the size distribution were used to discuss the possible exchange mechanisms.

Introduction

The micellar structure[4−11] and dynamics[12−20] of many poly(ethylene oxide)−poly(propylene oxide)−poly(ethylene oxide) (PEO-PPO-PEO) triblock copolymers, have been extensively investigated throughout the past decade using various techniques.[1−20] Among these systems are Pluronics, Polaxamers, and Synperonics. This information is very useful for many applications such as controlled drug delivery, pharmaceutical formulation, cosmetics, bioseparation, and extraction.[1−3] Despite the large amount of publications on the characterization of Pluronic systems, several issues are still unsolved concerning the micellization process close to the critical micelle temperature (cmT)[4−7] and micellization dynamics.[19]

Most of our knowledge about micelle dynamics comes from chemical relaxation experiments.[21] In these experiments the system is rapidly perturbed to a nonequilibrium state by changing the temperature, pressure, or surfactant concentration. The relaxation to equilibrium is monitored through observation of the conductivity if the system is ionic, or by light scattering, circular dichroism, or fluorescence if the micelles are nonionic. In particular, in the dynamic experiment on Pluronic surfactants using a temperature jump "T-jump", the total scattered intensity is usually used to quantify the relaxation process.[12,19] Exchange experiments showed that many Pluronic surfactants such as L64 and P85 exhibit millisecond-type kinetics. These systems exhibit a behavior similar to that of many nonionic surfactants such as Triton-X100.[23] These measurements frequently identify two well-separated relaxation times, a rapid relaxation (τ_1) that occurs on a time scale of microseconds and a slower process (τ_2), which requires milliseconds to seconds or longer.

Aniansson and Wall[22] attributed the fast process to an association−dissociation mechanism involving the exchange of individual surfactant molecules between the micelles and the water phase. This affects the size of the micelles without changing their number. On the other hand, there are several interpretations for the slow process. The slow process was described by Aniansson and Wall (AW) as being due to the re-establishment of equilibrium through cooperative condensation or dissolution of surfactant monomers.[22] This process results in the creation and breakdown of entire micelles and yields a change in both the micellar size and the number of micelles in solution. The AW mechanism only considers reactions involving aggregates and free surfactant molecules. Two other slow relaxation processes have been suggested in the literature.[23−32] One process involves the fusion of two micelles to form a transient "supermicelle," which subsequently fragments back to two normal micelles. The other mechanism involves the fragmentation of a normal micelle into two short-lived "submicelles," which grow back to normal micelles through fusion or through condensation of free surfactant monomers present in the solution. These mechanisms should exhibit a different dependence of the exchange rate (k_{obs}) on the micelle concentration. The fusion fragmentation process should exhibit a second-order kinetic with $k_{obs} = k_{ff}$•[micelle] (k_{ff} is the rate of fusion), whereas the fragmentation−growth process is expected to exhibit a first-order kinetic and a constant $k_{obs} = k_{fg}$ (k_{fg} is the rate of fragmentation growth). These two mechanisms have been directly identified in nonionic surfactants such as Triton X-100 and Synperonics, using the fluorescence stopped flow technique and highly hydrophobic pyrene probes.[26,31] Since these probes cannot migrate between micelles by exit and reentry via the aqueous phase, they exchange between the micelles by means of fusion and fragmentation.[26−31] Furthermore, molecular simulation also suggests that spontaneous fragmentation growth is an important mechanism during the micelle formation process.[32]

In most of the kinetic experiments on Pluronics using temperature jump, the total scattering intensity is usually used to monitor the micellization kinetics.[12−20] The total scattering intensity is a combination of many parameters of the micelle

* To whom correspondence should be addressed. E-mail: rharbi@ujf-grenoble.fr.
[†] Laboratoire de Rhéologie, UJF/INPG/CNRS.
[‡] Universidad de Guadalajara.

10.1021/jp809685q CCC: $40.75

structure: size, size distribution, and water content. During the relaxation process all these parameters could vary simultaneously and thus the quantitative analysis of the process should consider the variation of each parameter during the experiment. In the particular case of "T jump" experiments on Pluronic solutions, the scattering intensity increases in the fast process (first process) and then either decreases in the slow process (second process) at moderate temperature above cmT or increases again (third process) at high temperatures. The first process is associated with incorporation of free copolymer in the micelles, which yield metastable micelles. The second process was attributed to the reorganization of the metastable micelles through various possible correlated processes: dehydration of the micelles, change of the size of the micelles, and their aggregation number as well as the evolution of the size distribution.[18] Therefore, in order to develop the appropriate dynamic model, one should directly measure the temporal evolution of the size distribution of the micelles throughout the kinetic experiment.

A few experiments using high-flux X-ray scattering combined with stopped flow have been performed to measure the shape evolution of the surfactant micelles.[33] Similar experiments have been carried out using the neutron scattering technique.[34] Since these techniques are not easily accessible, the majority of the dynamic experiments described in the literature do not directly measure the average micellar size and the size distribution during the kinetic but rather assume them.[19] Several questions still remain unanswered regarding how the fragmentation process affects the size distribution and what is the result of fragmentation. Thus, there is a need for an experiment where the size distribution, the average micelle size, and the size polydispersity as well as the total scattering intensity are measured throughout the kinetic experiment.

In this report, we investigate the relaxation kinetics of Pluronic P103 by means of dynamic light scattering (DLS). The properties of the micelles were investigated throughout the relaxation kinetic of micelles, following a change in the temperature. The solutions were equilibrated at a given temperature before measurement and were then rapidly transferred to the measurement cell, which was set at another temperature. Since Pluronic P103 exhibits minute-type kinetics, it is a good candidate for carrying out kinetic experiments using DLS. The scattering intensity and the hydrodynamic radius as well as the size distribution were measured during the kinetic experiments using DLS. These parameters were used to obtain insight into the exchange dynamics of the P103 micelles.

Experimental Section

Materials. The triblock copolymer Pluronics P103 (batch 1, Polioles SA de CV) and the P103 (batch 2, BASF Corp.) were used as received. The Pluronic P103 ($PEO_{17}PPO_{60}PEO_{17}$) has a $M_w = 4.95$ kg/mol. Doubly deionized water was used in the preparation of solution. Aqueous Pluronic solutions were prepared by mixing the copolymer with water under gentle agitation at room temperature for more than 24 h. The Pluronic P103 was also purified in hexane by washing 1 g of pure P103 with 10 mL of hexane at 26 °C for 1 h.[35] This procedure was repeated 3 times and the P103 was then dried at 50 °C to remove the residual hexane.

Fourier transform infrared spectroscopy (FTIR) experiment on the raw and purified P103 was carried out on Perkin-Elmer spectrum 100 FT-IR on BaF2 window.

Dynamic Scanning Calorimetry. Thermograms were obtained with a TA Instruments-Q100 differential scanning calorimeter (DSC) that had been previously calibrated with indium, water, and *n*-octane standards. All scans were done with heating rates of 10 °C/min. Aluminum pans for volatile samples (TA Instruments) were employed to minimize loss of water by evaporation. Samples in the sealed pans were weighed before and after each test. Results from samples that lost weight were discarded.

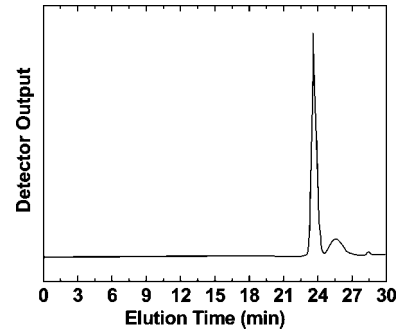

Figure 1. GPC detector output versus elution time for P103.

Gel Permeation Chromatograph (GPC). Molecular weight distribution was performed using a Packard-1110 gel permeation chromatograph (GPC) equipped with a refractive index detector in HPLC-grade tetrahydrofuran (THF, Merck) at a flow rate of 1 mL/min and three PL Gel columns with exclusion sizes of 10^3, 10^4, and 10^5 Å. The universal calibration curve, obtained with polyethylene oxide standards, was used directly to calculate the molar masses of the P103 components.

Gas permeation chromatography on the P103 samples showed two main peaks (Figure 1). The strong peak is attributed to the triblock P103 copolymer with a $M_w = 4.95$ kg/mol, while the small peak at 26 min corresponds to small macromolecules with $M_w = 1.37$ kg/mol. The details of the GPC analysis of the Pluronic P103 were also developed by Nolan et al.[5] They found the P103 to be composed of more than one population and estimated the fraction of the impurity to be around 13%. The small peak is attributed to more hydrophobic macromolecules.[41] These copolymers are often studied or used in various applications without further purification, and therefore one needs to understand the dynamic of the raw copolymer in order to develop a consistent comparison with the literature studies.

Dynamic Light Scattering. Dynamic light scattering (DLS) measurements were done on a Malvern Zetasizer 4000 apparatus equipped with a 7132 Multibit correlator and multiangle goniometer. The light source was a 5mW He−Ne laser with wavelength of 633 nm. Light scattering measurements on micelles at equilibrium were carried out at various angles 70, 90, 110, and 130°, and the results were averaged over 10 measurements. The total scattering intensity is measured during the DLS experiment through a pinhole of 400 μm at 90°.

All the samples were left at the desired temperature from 1 h up to 12 h prior to the measurement depending on the kinetics of the system. The criterion used to define when the structure reached equilibrium was when the total scattering intensity remained constant with time. To characterize the structure of the micelles, DLS measurements were performed for 30 s and repeated 10 times.

The Correlation functions $g^2(q,t)$ of the scattering light intensity were analyzed following[36]

$$g^2(q,t) = 1 + [\beta \int \exp(-t/\tau)P(\tau)\,d\tau]^2 \qquad (1)$$

using the CONTIN routine, where $P(\tau)$ is the distribution function of the relaxation time and the coherent factor of the

instrument $\beta \approx 1$.[37] The corresponding hydrodynamic radius is calculated using the Stokes−Einstein equation.

$$R_H = \frac{k_B T}{6\pi\eta} q^2 \tau(q) \quad (2)$$

In other analysis the correlation function is analyzed using the cumulants method.[36]

$$\ln |g^2(q,t)| = -\Gamma t + \frac{1}{2!}\mu_2 t^2 - \frac{1}{3!}\mu_3 t^3 + ... \quad (3)$$

where Γ is the first cumulant being $\langle\Gamma\rangle = q^2 D$, where D is the diffusion coefficient. These results were used to estimate the hydrodynamic radius:

$$R_H = \frac{k_B T}{6\pi\eta D} \quad (4)$$

The scattering intensity can be written as

$$I_{scat} \propto (n_{mic} - n_w)^2 / V \sum_i P^i_{mic} (V^i_{mic})^2 \quad (5)$$

where V^i_{mic} and P^i_{mic} are the volume and the fraction of micelles containing "i" surfactant molecules and V is the total volume of the solution. The n_{mic} and n_w are the refractive indices of the micelles and water, respectively.

Kinetic Experiment. The kinetic measurements were performed using a nonstandard procedure: the surfactant solution in a 10 mm cylindrical glass cell was first equilibrated at a given temperature (T_{peak}) for 12 h in a temperature-controlled bath. The sample was then rapidly transferred into the DLS sample holder, which had been previously set at a temperature (T_2) and the DLS measurements were then started immediately. The measurement time for each autocorrelation decay was fixed for 5 s, and measurements were carried out continuously until the apparent hydrodynamic radius and the total intensity reached constant values. All the kinetic measurements were performed at an angle of 90°.

Throughout the kinetic experiment, the measurement cell was gently agitated with a mini-agitator and the temperature of the Pluronic solution in the cell was measured using a thin thermocouple. In our experimental conditions, the temperature inside the measurement cell reached 97% of the desired temperature within 1.5 min. We can thus safely quantitatively consider the kinetic experiment for [P103] < 2%, and we exploit qualitatively the results of experiments for [P103] > 2%.

We performed kinetic experiments by carrying out a temperature jump from a temperature T_{peak}, which yields large aggregates to a temperature $T_2 = 26$ °C. T_{peak} is around the cmT and varies between 22 and 17 °C for [P103] between 0.25 and 3 wt %. This allowed the study of the kinetics of formation of proper micelles from premicellar aggregates. The temporal evolution decays of the scattering intensity and the apparent hydrodynamic radius were fitted with a monoexponential expression.

Results and Discussion

Micelle Structure of the Aqueous P103 Solutions. In order to efficiently comprehend the kinetics of P103 micelles, we first investigate their structure at various temperatures using dynamic light scattering. The experiments were carried out on copolymer solutions which had been previously equilibrated at a desired temperature for more than 12 h. In Figure 2a we show the variation of the total scattering intensity (I_{scat}) and the hydrodynamic radius (R_H) for 3 wt % P103 solution as a function of temperature. Below the critical micelle temperature (cmT), the total intensity is low and corresponds to a solution of individual P103 monomers (and impurities) in water. Close to cmT, both R_H and the I_{scat} increase and then decrease giving a peak at 19 °C for 3 wt % and 21 °C for 1 wt %. The I_{scat} and R_H at the peak are independent of the scattering angle, which infers that the aggregates are isotropic objects (Figure 2b). If the aggregates were anisotropic, R_H and I_{scat} would decrease with increasing scattering angle. As the temperature increases above cmT the large aggregates "premicelles" become proper spherical micelles. The temperature of the peak (T_{peak}) is found to be around the critical micellization temperature cmT from the literature[2,4] and it decreases with increasing [P103] from 24 °C for 0.25 wt % to 19 °C for 3 wt % (Figure 3). At T_{peak}, the P103 form large aggregates with an apparent hydrodynamic radius R_H in the order of 35 nm. The general behavior of the peak and the value of T_{peak} were found to be reproducible in both the P103 batches (Polioles and BASF) (Figure 3b). The peak intensity occurs in the beginning of the micellization process and superimpose with the rising region of the DSC thermograph. Beyond the peak intensity, the aggregates give place to proper micelles which grow by condensation of the free surfactant unimers (Figure 4a). The size of the proper micelles increases slowly at high temperatures and above 35 °C increases rapidly as the temperature approaches the cloud point.

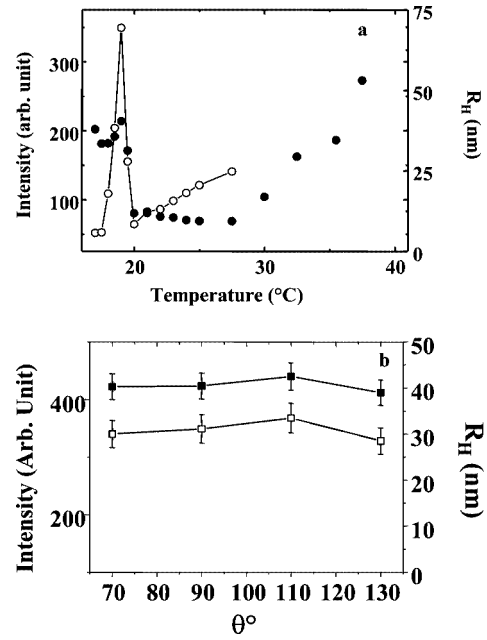

Figure 2. (a) Light scattering intensity I_{scat} (□) and the hydrodynamic radius R_H (■) plotted vs temperature for 3 wt % P103 solution in water. (b) Light scattering intensity (I_{scat}) and the hydrodynamic radius R_H, measured at the peak temperature, plotted vs the scattering angle for 3 wt % P103 solution in water.

In order to understand the origin of the peak intensity, we purified the Pluronic P103 by washing 1 g of pure P103 with 10 mL of hexane at 26 °C for 1 h.[35] This procedure was repeated 3 times and the P103 was then dried at 50 °C to remove the residual hexane. This procedure allowed the removal of the more hydrophobic components from the P103. The hexane solution

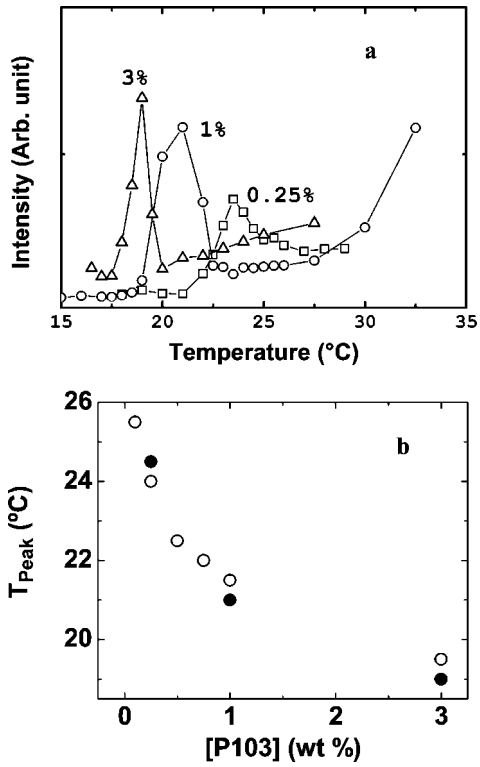

Figure 3. (a) Scattering intensity (I_{scat}) vs temperature for P103 solution with concentration 0.25, 1, and 3 wt %. (b) The temperature corresponding to the peak T_{peak} plotted vs the concentration of P103 for batch 1 (○) and batch 2 (●).

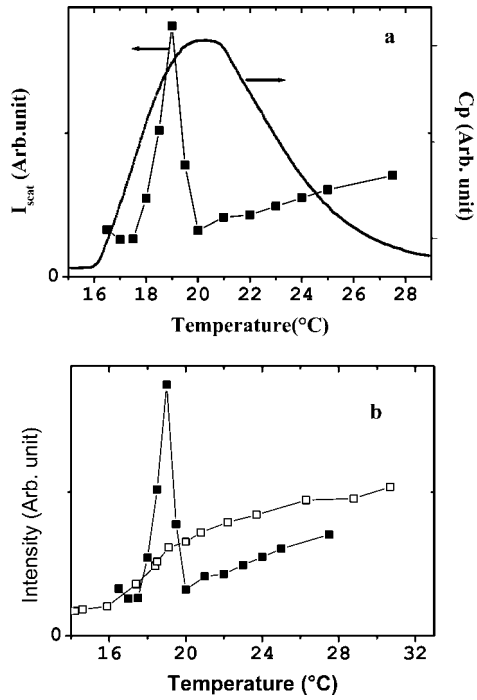

Figure 4. (a) I_{scat} and the DSC thermograph of 3 wt % P103 solution in water. (b) Scattering intensity (I_{scat}) vs temperature for 3 wt % P103 solution before purification (■) and after purification in hexane (□).

was evaporated to extract the hydrophobic impurity. FTIR results on the raw P103, the purified, and the impurities were analyzed based on the position of the absorption peaks of the PPO and P103 from ref 10. The impurities were found to be mainly composed of PPO molecules. In Figure 4b, we compare the scattering intensity of P103 solution before and after purification. The scattering peak disappears after purification of the P103, which infers that hydrophobic impurities initiate the formation of the large aggregates and the large scattering peak. In the proximity of the cmT, the hydrophobic impurities probably initiate the formation of large aggregates (premicelle clusters) containing mixtures of surfactant P103 and impurities.[35] Similar peaks in the scattering intensity have been reported in the Pluronic L64 in the vicinity of cmT.[35] When the L64 was purified in hexane, the peak disappears and was found to reappear when impurities of hydrophobic oligomers of the same PPO length (L61) were added to the solution.

A recent study by Liu et al.[4] reported that R_H of P103 increases 2−3 times upon cooling the solutions below the cmT. They reported that the magnitude of increase of R_H is different with cooling and heating. We found that the kinetic of aggregate formation upon cooling is slow (more than 3 h) and if Figure 2a is repeated with a fast scan of the temperature, we do not clearly observe the formation of the premicelle aggregates. Recently, Nilsson et al.[7] investigated the effect of copolymer polydispersity on the micellization of a more hydrophilic copolymer (F127) and proposed that the hydrophobic fraction of the copolymer takes part in the micellization process while the hydrophilic part remains free and as the temperature increases the more hydrophilic parts associate with the micelles.

If the solutions are not filtered, the R_H increases with decreasing temperatures for temperatures below the T_{peak}. The scattering intensity of the aggregates below T_{peak} is low, which infers that the fraction of these aggregates is negligible and is easily eliminated by filtering the solutions prior to DLS measurements.

Kinetic Experiments. Traditionally the T-jump experiment is carried out by inducing a 1 °C jump in the temperature within a few microseconds using an iodine laser. Our experiment, however, uses a different procedure where the temperature is increased by 3 to 10 °C from T_{peak}, which yields large aggregates ($R_H \approx 35$ nm) to 26 °C, which gives spherical proper spherical micelles (Figure 2a). The evolution kinetics from aggregates to proper micelles is monitored by DLS, where the total scattering intensity (I_{scat}), the hydrodynamic radius (R_H), and the size distribution are measured during the kinetics.

Kinetic Experiments Using the Total Scattering Intensity and Comparison with the T-Jump Method. In Figure 5a we show the decay of the total scattering intensity (I_{scat}) vs time for 1 wt % P103 solution after the temperature has been rapidly changed from T_{peak} to 26 °C. The scattering intensity increases in the first 2 min and then decreases during the next 30 min. This means that the kinetic is composed of two processes: a fast process in which I_{scat} increases and a slow process in which I_{scat} decreases. The decay of the fast process cannot be analyzed quantitatively because it is faster than the rate of increase of the temperature. The increase of I_{scat} in the fast process is most likely due to condensation of free copolymers into the premicelle aggregates and to partial dehydration of the aggregates. Indeed, increasing the temperature from T_{peak} to 26 °C yields (1) a decrease of the free copolymer concentration, which incorporates the aggregates, and (2) a reduction of the water content of the aggregates,[8,10] which increases the micelle/water contrast and enhances I_{scat}. In the beginning of the kinetic process, the copolymer unimers incorporate the aggregates, which then undergo a slow kinetic process to give spherical proper micelles. In Figure 5b we show the slow kinetic decay of I_{scat} vs time for [P103] ranging from 0.25 to 3 wt %. These decays were found to fit well to a single-exponential equation (Figure 5), with a relaxation time (τ) varying between 500 and 1.7 min for [P103]

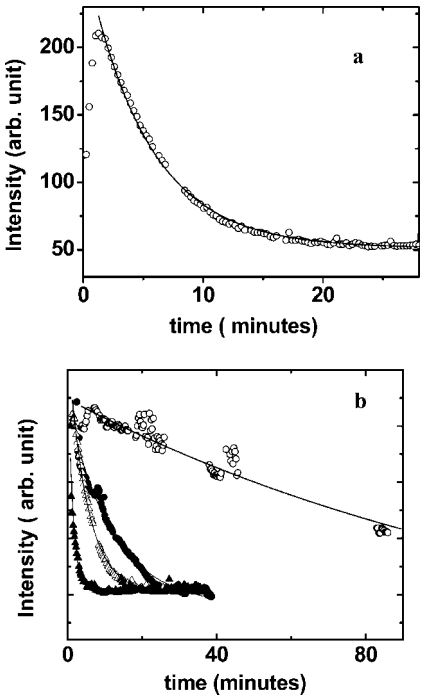

Figure 5. Scattering intensity vs time for various aqueous P103 solutions after the solution was transferred from a temperature T_{peak}, which yield a peak in the scattering intensity to $T_2 = 26$ °C. (a) The decay of I_{scat} vs time for [P103] = 1%. (b) The decays of I_{scat} vs time for [P103] = 0.5% (○), 0.75% (●), 1% (△), and 1.5% (▲). The decays are fitted to a single-exponential expression (solid line).

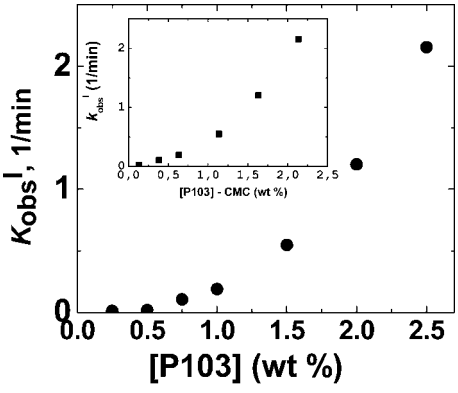

Figure 6. Exchange decay k^I_{obs} calculated from fitting the decays of the scattering intensity (I_{scat} vs time) (Figure 5) to a single-exponential expression, plotted against the concentration of P103 (batch 1). (Inset) k^I_{obs} plotted against [P103] − cmc. The cmc is taken from ref 40 to be cmc = 0.366 wt %.

ranging from 0.25 to 1.5 wt %. The good fit of these decays to the single exponential could mean that the exchange mechanism is a first order or a pseudo-first-order process. In the case of a first order or pseudo first order, the decay can be calculated as $dI_{scat}/dt = -k_{obs}I_{scat}$, with the decay rate k_{obs} independent of I_{scat}, which yields an exponential decay.

$$I_{scat}(t) = A \exp(-t/\tau) + I_{scat}(\infty) \tag{6}$$

Figure 6 depicts the rate of the kinetic $k^I_{obs} = 1/\tau$ calculated from the decay of the I_{scat} as a function of [P103]. For [P103] < 0.5% the k^I_{obs} increases slowly with increasing [P103], whereas for [P103] > 0.5 wt %, k^I_{obs} increases linearly with [P103]. When the experiment was repeated with P103 batch 2 (BASF), the k^I_{obs} vs [P103] followed exactly the same behavior as batch 1. However, the k^I_{obs} in batch 2 is found to be 3 times larger than that of batch 1. This infers that the mechanism controlling the dynamics depends mainly on the structure of the copolymer, whereas the magnitude of the dynamic rate depends on the small compositional differences between different copolymers. This is supported by the results reported elsewhere,[35] which suggest that addition of hydrophobic impurities slows down the dynamics of Pluronic L64.

We should point out that the micellization is not complete at 26 °C and a fraction of the P103 remains free in the aqueous phase ($[P103]_{free}$). The $[P103]_{free}$ could be considered equal to the critical micelle concentration (cmc). The cmc was estimated at 25 °C to be cmc = 0.366 wt % using iodine/iodide absorption[40] and 0.07% using 1,6-diphenyl-1,3,5-hexatriene absorption.[14] To take into consideration only the fraction of micellized copolymer, we replotted k^I_{obs} against [P103] − cmc, using the highest value of cmc = 0.366 wt % (Figure 6, inset). The shape of this plot is not different from that of Figure 6 and therefore taking into consideration the micellized part of the copolymer did not drastically change the shape of the k^I_{obs}.

In the literature, T-jump experiments on Pluronic triblock copolymers such as L64 [19,20] and F85[16] show two clear exchange kinetics: a fast kinetic and a slow one. The scattering intensity was found to increase in the fast process and then either decrease in the slow process (second process) at moderate temperatures above cmT or increase again (third process) at high temperatures. The first process is associated with incorporation of free copolymer in the micelles which yields metastable large micelles. The second process was assigned to the reorganization of the metastable micelles.[19] The exchange kinetic in our experiment, when monitored using the scattering intensity, is also composed of two processes. The second slow process likely corresponds to the second slow process in the T-jump experiment on L64 and F85[15−20] due to similarities between the two: (1) the scattering intensity decreases in both kinetics and (2) they yield a similar dependence of k^I_{obs} on the surfactant concentration (Figure 6 and ref 19). There are, nonetheless, some differences between these two experiments: (1) the kinetic in the T-jump is monitored following a small variation in temperature $\Delta T = 1$ °C, whereas in our experiment ΔT ranged from 3 to 10 °C; (2) the second slow process in the T-jump occurs on metastable large micelles which are formed in a short time scale during the first process, whereas the exchange in the present experiment occurs on thermodynamically stable P103 aggregates formed at T_{peak}. Though the two kinetic experiments are performed under different conditions, they yield a similar dependence of k_{obs} on surfactant concentration and therefore they are likely to involve similar mechanisms: (1) dehydration of the micelles, (2) cooperative condensation and dissolution of monomers, and (3) fusion-fragmentation process or fragmentation and growth process.

Kinetics of Micelle Size. The total intensity contains information about the average micelle size, the polydispersity, and the size distribution as well as the water content of the micelles. For monodispersed micelles, the scattering intensity (eq 5) could be written as

$$I_{scat} \propto (n_{mic} - n_w)^2 \phi_{mic} V_{mic} \tag{7}$$

where V_{mic} is the volume of the micelle and φ_{mic} is the volume fraction of the micellized surfactant. During the relaxation process, all these parameters could vary simultaneously, which would complicate the description of the dynamic process.

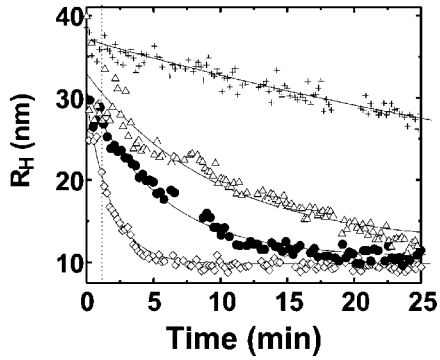

Figure 7. Hydrodynamic radius plotted against time after the solution was transferred from T_{peak} to $T_2 = 26$ °C. The concentration of the polymer was [P103] = 0.5% (+), 0.75% (Δ), 1% (●) and 1.5% (◇). The decays are fitted to a single-exponential expression (solid line).

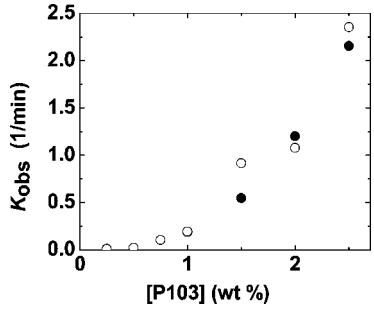

Figure 8. Exchange decay k_{obs} calculated from fitting the decays of (R_H vs time) (Figure 3) to a single-exponential expression, plotted against the concentration of P103. k_{obs} calculated from R_H (○) is compared to k^I_{obs} calculated from the scattering intensity (●).

Therefore, the variation of each of the micelle parameters should be monitored individually. In Figure 7 we show the change in the hydrodynamic radius (R_H) with time for various [P103]. R_H is calculated from the cumulant method. Unlike the I_{scat} decay, the R_H decay is only composed of the slow process and the fast process is not observed. This infers that the fast process in our system most likely involves two counterbalancing processes: (1) condensation of the free copolymers in the aggregates, which increases the aggregation number and (2) dehydration, which reduces the size.

The decays of R_H vs time fit reasonably to a single-exponential expression. As mentioned before, the good fit of these decays to the single exponential could mean that the exchange mechanism is a first-order or a pseudo-first-order process.

$$R_H(t) = A \exp(-t/\tau) + R_H(\infty) \tag{8}$$

The rate of the kinetic calculated from the decays of R_H is $k^{RH}_{obs} = 1/\tau$. The plot of k^{RH}_{obs} vs [P103] is found to be superimposable with the plot of k^I_{obs} for the whole range of [P103] investigated here (Figure 8).

When the temperature increases from T_{peak} to 26 °C, the cmc decreases and thus part the free P103 molecules associate with the aggregates, leading the intensity to increase in the early part (2 min) of the exchange kinetic (Figure 5a). Beyond this time, the decrease in R_H and the I_{scat} can be solely attributed to dynamic mechanisms involving aggregates and proper micelles. Similarly, the fast process in the conventional T-jump experiment is associated to condensation of the surfactant in the micelles to form metastable large micelles, which then undergo slow exchange mechanisms to reach equilibrium.

The exchange kinetics in Pluronics could involve the change in various parameters: the number of copolymers per micelle (N_{agg}), the size distribution, or even the water content.[19] If the kinetic experiments were only to involve the variation of N_{agg}, then $I_{scat} \propto N_{agg} \propto V_{mic} \propto R_H^3$ (eqs 5, 6, and 7) and in the case of exponential decays $k^I_{obs} = 3k^{RH}_{obs}$. However, since $k^I_{obs} = k^{RH}_{obs}$, we can conclude that the kinetic from aggregates to proper micelles involves the change in other parameters in addition to the variation of the aggregation number, such as the refractive index and the size distribution.

Small-angle neutron scattering experiments on the Pluronic P85 have shown that micelles close to cmT contain up to 60% water in 5% P85 at 32 °C.[8] Similar conclusions were also reported on P103 micelles using Fourier transform infrared spectroscopy.[10] The amount of water in the micelles has been reported to decrease with increasing temperature.[8,10] Since there is an increase in temperature in our experiments, the micelles likely dehydrate during the kinetic experiment.[8,38,39] To take into consideration the change in water content of the micelles, the refractive index of the micelle can be written as $n_{mic} = an_{P103} + (1 - a)n_w$ assuming that the water repartition in the PPO core and the PEO corona is uniform, where n_{P103} is the refractive index of pure P103 and a is the fraction of P103 in the micelles. The scattering intensity can then be written as

$$I_{scat} \propto a^2(n_{P103} - n_w)^2 \phi_{mic} V_{mic} \tag{9}$$

The fraction of P103 in the micelle can be written as $a \propto N_{agg}/V_{mic}$, where N_{agg} is the number of P103 in the micelle (aggregation number) and thus eq 9 becomes

$$I_{scat} \propto (n_{P103} - n_w)^2 \phi_{mic} (N_{agg}/V_{mic})^2$$

$$I_{scat} \propto (N_{agg})^2/V_{mic} \tag{10}$$

If the kinetics were only to involve dehydration and the N_{agg} were to remain constant, the scattering intensity would increase with time when R_H decreases since $I_{scat} \propto 1/R_H^3$. Therefore, since I_{scat} was found to decrease with time (Figure 5), dehydration cannot be the only mechanism involved in this exchange kinetic. Furthermore, dehydration involves only the interaction of water with the surfactant molecules and thus one would expect it to yield a rate independent of surfactant concentration. The increase of k_{obs} with increasing [P103] (Figure 6) is in disagreement with the idea that dehydration dominates the kinetic process. Hence, from the above argument, we can conclude that the exchange kinetic involves a decrease in both the water content and the aggregation number of the micelle. In order to obtain $k^I_{obs} = k^{RH}_{obs}$ using eq 10 ($I_{scat} \propto N_{agg}^2/R_H^3$), the N_{agg} should decrease at a rate of $k_{Nagg} = 2k^I_{obs}$. From eq 10, we can estimate the water content of micelle to decrease at a rate of $k_w = k^I_{obs}$.

Kinetic of the Size Distribution. When taking into consideration the micelle polydispersity, the scattering intensity can be described by eq 5. The way in which the size distribution (P^i_{mic}) of micelles evolves during the relaxation dynamic remains a major question. Experiments involving high-flux small-angle X-ray scattering or neutron scattering measurements synchronized with stopped flow mixing were found to give information on the temporal evolution of the micellar structure.[33,34] Since our kinetics for low [P103] is sufficiently slow to carry out the DLS experiments, we used CONTIN analysis to obtain the size

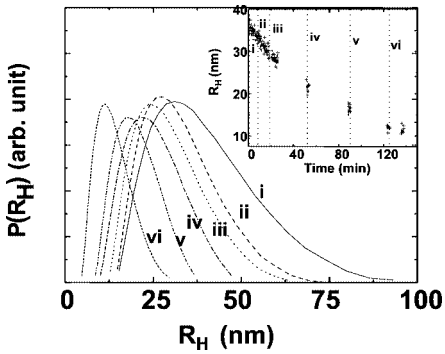

Figure 9. Size distribution of P103 solution (0.5 wt %) at various times during the exchange kinetics following a temperature jump between T_{peak} and $T_2 = 26$ °C. (Inset) The average hydrodynamic radius R_H vs time during the exchange kinetic of the 0.5 wt % P103 solution. The broken lines in the inset indicate the time at which the size distribution is presented in Figure 9.

distributions throughout the exchange process. Figure 9 depicts the size distributions of micelles for 0.5 wt % P103 aqueous solution at various times during the kinetic experiment. The inset of Figure 9 shows the corresponding time for each size distribution curve. This plot shows that both the average size and the width of the size distribution decrease during the kinetic process. In Figure 10 we show the average micelle size and the width of the size distribution (σ) vs time, where σ was calculated from the full width at half-maximum (fwhm) of the size distribution (Figure 9) as σ = fwhm/2.3458. These two plots follow the same behavior and therefore one can conclude that the relative polydispersity (σ/R_H) of these micelles remains constant during the whole kinetic process, which means that the width of the distribution remains proportional to the size of the micelles (Figure 11).

Mechanisms for the Micellization Dynamics. The kinetic in this system involves dehydration and exchange of P103 molecules between micelles in the slow kinetic process. Several possible mechanisms could explain the exchange kinetics of P103 copolymers between micelles. One possibility is cooperative condensation and dissolution of monomers, which was proposed by Annianson and Wall.[22] This process involves the creation and breakdown of entire micelles and results in a change in both the micellar size and the number of micelles present in solution. This mechanism only applies to reactions involving aggregates and free surfactant molecules. According to this mechanism, free copolymer surfactants dissociate from large aggregates and associate to form spherical proper micelles. Hence the number of proper micelles increases at the expense of the large aggregates which diminish in number or size. This process should yield two populations of large and small micelles or at least a noticeable distortion of the size distribution and a change in the relative polydispersity during the kinetic process. However, the relative polydispersity of our system remains practically invariant during the kinetics, which is in disagreement with this mechanism.

Another possible mechanism to explain the P103 copolymers exchange kinetics is "fragmentation−growth". In this process, aggregates fragment into two submicelles, which then grow into proper micelles either via fusion or association of free surfactant molecules.[23−32] The fragmentation mechanism is a unimolecular process and thus should give a first-order kinetic. A first-order or pseudo-first-order kinetic would lead to a single-exponential expression, whereas a second-order kinetic in our system would yield a complicated expression. The good fit of the decays to a single-exponential expression for all the concentrations investigated here supports the idea that the kinetic process is first order and reinforces the hypothesis that the kinetics is controlled by fragmentation.

On the other hand, fragmentation is a unimolecular process and thus should yield a constant $k_{obs} = k_{fg}$ (k_{fg} being the rate of fragmentation). However, the exchange rate k_{obs} was found to increase with increasing [P103], which would lead us to rule out fragmentation as the controlling mechanism and attribute the exchange to a second-order kinetic process. It is possible that though the kinetic is controlled by fragmentation, k_{fg} increases with increasing [P103]. A similar case has been observed in sodium dodecyl sulfate (SDS), where the rate of fragmentation at low [SDS], measured directly using fluorescence stopped flow, was found to increase with increasing [SDS] and increasing ionic strength.[29] In these experiments, the linear increase of k_{obs} with increasing [SDS] could have been interpreted as a fusion process; however, Rharbi and Winnik showed that an increase in [SDS] leads to increasing ionic strength and thus increasing the rate of fragmentation.[29]

An alternative mechanism is that fragmentation events are initiated after collision of two micelles i.e., "collision−fragmentation" (Scheme 1). The collision processes do not lead to fusion because of the steric barrier but they generate the energy necessary for the fragmentation of aggregates. In contrast with the previous model where fragmentation occurs spontaneously using the thermal energy of the micelle,[32] fragmentation in the collision−fragmentation process requires the energy resulting from the collision of two micelles. This mechanism is a second-order process and thus should yield an increase in k_{obs} with increasing [P103]. However, in contrast with the fragmentation mechanism that gives exponential decays of I_{scat}, developing an analytical expression for the temporal evolution of I_{scat} or R_H, using the collision−fragmentation process would require further details about the product of fragmentation.

The collision−fragmentation process could take place via various possible ways (Scheme 2):

1. One could imagine that thermodynamically stable small proper micelles detach from the aggregates successively during fragmentation (Scheme 2a). According to this process, when the micelles detach from the aggregates, they are already within the final size distribution of the micelles. This process would lead to two populations of micelles: a population of small proper micelles that increase at the expense of the large aggregates, which shrink. In the best case, one would observe a distortion of the size distribution and a modification of the relative polydispersity during the exchange kinetics. This mechanism disagrees with the observed evolution of the size distribution, i.e., one population of micelles with the same relative polydispersity.

2. The other possible mechanism involves successive fragmentation events of aggregates into two micelles of any size until the thermodynamically stable size is obtained (Scheme 2b). In contrast with the previous mechanism, where stable proper micelles detach from the aggregates, the present fragmentation mechanism gives micelles of any size. These micelles then grow via fusion with other micelles or via association with free monomers to form thermodynamically stable proper micelles. This mechanism can describe the observed evolution of the size distribution, where the average particle size decreases and the relative polydispersity remains constant. Therefore, a mechanism involving successive fragmentation of aggregates into micelles of any size could better describe the experimental results.

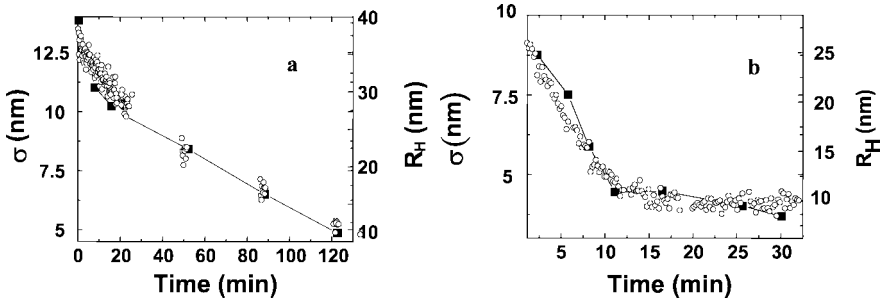

Figure 10. Comparison of the mean value of R_H, taken from the maximum of the size distribution (○) and the width of the size distribution (σ) (■) plotted vs time during the exchange kinetic of P103 solutions following a change in temperature between T_{peak} and $T_2 = 26$ °C. (a) 0.5 wt % P103 solution and (b) 1 wt % P103 solution. σ is calculated from the fit of the size distribution to a Gaussian distribution.

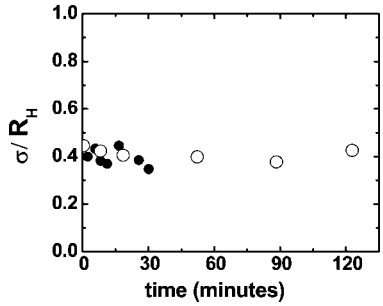

Figure 11. Relative polydispersity calculated as σ/R_H plotted vs time for P103 solutions at 0.5 wt % (○) and 1 wt % (●). σ is calculated from the fit of the size distribution to a Gaussian distribution.

SCHEME 1: Mechanisms for the Collision−Fragmentation Process

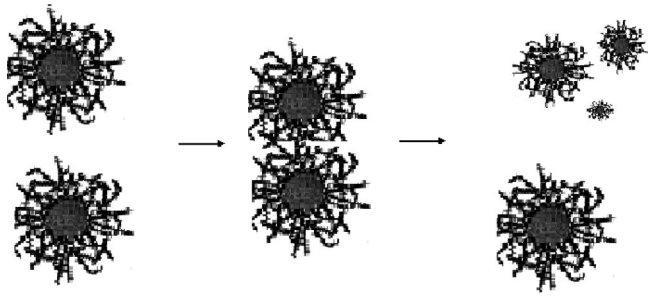

SCHEME 2: Possible Mechanisms for the Fragmentation

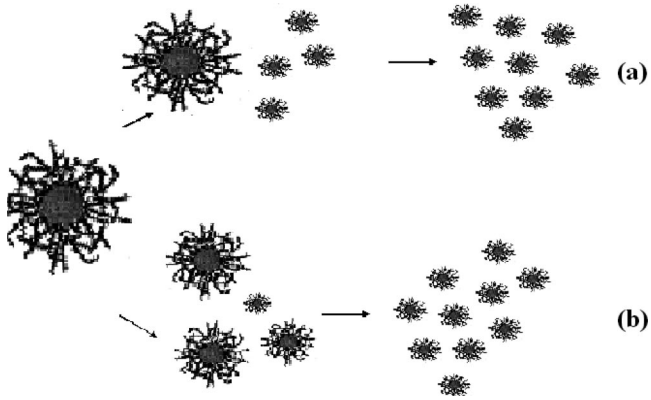

Conclusion

In this paper we study the exchange kinetic of aqueous solutions of the triblock copolymer Pluronic P103 surfactant from premicelle aggregates to proper micelles. We used dynamic light scattering to investigate the structure and the exchange kinetic of this system. Solutions of the P103 surfactant form large aggregates (35 nm) in the proximity of the critical micelle temperature (cmT), which results from interaction between triblock copolymer P103 and hydrophobic impurities of the system. At high temperatures the aggregates yield proper micelles. The kinetics of evolution from "aggregates" to "proper micelles" is investigated using DLS after a temperature jump. This method allowed us to measure the evolution of the scattering intensity, the average size, and the size distribution with time. The rate of change of the scattering intensity and the hydrodynamic radius were found to be similar which suggests that the exchange kinetic is accompanied by a dehydration process. Both the average size of the micelles and the width of the size distribution were found to decrease similarly with time, which suggests that the relative size polydispersity does not change during the kinetic process. Fragmentation is most likely the motor of the exchange kinetics. The increase in the exchange rate with increasing [P103] could either result from a fragmentation mechanism with a rate dependent on [P103] or from a mechanism involving collision−fragmentation. We propose that the fragmentation process, which yields any size micelles could better describe the temporal evolution of the size distribution.

Acknowledgment. This work was supported by the joint program ECOS-Nord M05P02E, MO6-P03 of the ministry of research and education (France) and the National Council of Science and Technology of México. We acknowledge Dr. Hélène Galliard for her valuable help in conducting these experiments, Mr. Joel Alfaro Hernàndez with his help in conducting the DSC experiment, and Mohamed Karrouch for his technical support.

References and Notes

(1) Schmolka, I. R. Poloxamers in the Pharmaceutical Industry. In *Polymers for Controlled Drug Delivery*; Tarcha, P. J., Ed.; CRC Press: Boca Raton, FL, 1991.

(2) Kabanov, A. V.; Batrakova, E. V.; Alakhov, V. Y. *Adv. Drug Delivery Rev.* **2002**, *54*, 759.

(3) Alexandridis, P. *Curr. Opin. Colloid Interface Sci.* **1996**, *1*, 490.

(4) Liang, X.; Guo, C.; Ma, J.; Wang, J.; Chen, S.; Liu, H. *J. Phys. Chem B* **2007**, *111*, 13217.

(5) Nolan, S. L.; Phillips, R. J.; Cotts, P. M.; Dungan, S. R. *J. Colloid Interface Sci.* **1997**, *191*, 291.

(6) Duval, M.; Waton, G.; Schosseler, F. *Langmuir* **2005**, *21*, 4904.

(7) Nilsson, M.; Hakansson, B.; Soderman, O.; Topgaard, D. *Macromolecules* **2007**, *40*, 8258.

(8) Goldmints, I.; Gottberg, F. K.; Smith, K. A.; Hatton, T. A. *Langmuir* **1997**, *13*, 3659.

(9) Goldmints, I.; Yu, G.; Booth, C.; Smith, K. A.; Hatton, T. A. *Langmuir* **1999**, *15*, 1651.

(10) Su, Y.; Wang, J.; Liu, H. Z. *J. Phys. Chem. B* **2002**, *106*, 11823.

(11) Almgren, M.; Alsins, J.; Bahadur, P. *Langmuir* **1991**, *7*, 446.

(12) Yang, L.; Alexandridis, P.; Steytler, D. C.; Kositza, M. J.; Holzwarth, J. F. *Langmuir* **2000**, *16*, 8555.

(13) Alexandridis, P.; Hatton, T. A. *Colloids Surf. A* **1995**, *96*, 1.

(14) Alexandridis, P.; Holzwarth, J. F.; Hatton, T. A. *Macromolecules* **1994**, *27*, 2414.
(15) Waton, G.; Michels, B.; Zana, R. *J. Colloid Interface Sci.* **1999**, *212*, 593.
(16) Michels, B.; Waton, G.; Zana, R. *Colloids Surf. A* **2001**, *183*−*185*, 55–65.
(17) Goldmints, I.; Holzwarth, J. F.; Smith, K. A.; Hatton, T. A. *Langmuir* **1997**, *13*, 6130.
(18) Michels, B.; Waton, G. *Langmuir* **1997**, *13*, 3111.
(19) Kositza, M. J.; Bohne, C.; Alexandridis, P.; Hatton, T. A.; Holzwarht, J. F. *Macromolecules* **1999**, *32*, 5539.
(20) Waton, G.; Michels, B.; Zana, R. *Macromolecules* **2000**, *34*, 907.
(21) For reviews of dynamic processes in micelles, see: (a) Muller, N. In *Solution Chemistry of Surfactants*; Mittal, K. L., Ed.; Plenum: New York, 1979; Vol. I, pp 267−295. (b) Gormally, J.; Gettins, W. J.; Wyn-Jones, E. In *Molecular Interactions*; Wiley: New York, 1980; Vol. 2, pp 143−177. (c) Lang, J.; Zana, R. In *Surfactant Solutions: New Methods of Investigation*; Zana, R., Ed.; Marcel Dekker: New York, 1987; pp 405−452. (d) Huibers, P. D. T.; Oh, S. G.; Shah, D. O. In *Surfactants in Solution*; Chattopadhay, A. K., Mittal, K. L., Eds.; Marcel Dekker: New York, 1995; Vol. 64, pp 105−121.
(22) (a) Aniansson, E. A. G.; Wall, S. N. *J. Phys. Chem.* **1974**, *78*, 1024; **1975**, *75*, 857. (b) Aniansson, E. A. G.; Wall, S. N.; Almgren, M.; Hoffmann, H.; Kielmann, H.; Ulbricht, W.; Zana, R.; Lang, J.; Tondre, C. *J. Phys. Chem.* **1976**, *80*, 905.
(23) Zana, R. In *Surfactants in Solution*; Mittal, K. L., Bothorel, P., Eds.; Plenum Press: New York, 1986; Vol. 4.
(24) Kahlweit, M. In *Physics of Amphiphiles, Micelles, Vesicles, and Microemulsions*; Degiorgio, V., Corti, M., Eds.; North Holland: Amsterdam, 1985.
(25) Kahlweit, M. *J. Colloid Interface Sci.* **1982**, *90*, 92.
(26) Rharbi, Y.; Li, M.; Winnik, M. A.; Hahn, K. G. *J. Am. Chem. Soc.* **2000**, *122*, 6242.
(27) Rharbi, Y.; Winnik, M. A.; Hahn, K. G. *Langmuir* **1999**, *15*, 4697.
(28) Rharbi, Y.; Winnik, M. A. *Adv. Colloid Interface Sci.* **2001**, *89*, 25.
(29) Rharbi, Y. M.; Winnik, M. A. *J. Am. Chem. Soc.* **2002**, *124*, 2082.
(30) Rharbi, Y.; Chen, L.; Winnik, M. A. *J. Am. Chem. Soc.* **2004**, *126*, 6025.
(31) Rharbi, Y.; Bechthold, N.; Landfester, K.; Salzman, A.; Winnik, M. A. *Langmuir* **2003**, *19*, 10.
(32) Rene', P.; Bolhuis, P. G. *Phys. Rev. Lett.* **2006**, *97*, 018302.
(33) Schmölzer, St.; Gräbner, D.; Gradzielski, M.; Narayanan, T. *Phys. Rev. Lett.* **2002**, *88*, 258301.
(34) Gradzielski, M.; Grillo, I.; Narayanan, T. *Prog. Colloid Polym. Sci.* **2004**, *129*, 32.
(35) Kositza, M. J.; Bohne, C.; Alexandridis, P.; Hatton, T. A.; Holzwarht, J. F. *Langmuir* **1999**, *15*, 322.
(36) Berne, B.; Pecora, R. *Dynamics Light Scattering*; Wiley: New York, 1976.
(37) Provencher, S. W. *Comput. Phys. Commun.* **1982**, *27*, 229.
(38) Wanka, G.; Hoffmann, H.; Ulbricht, W. *Colloid Polym. Sci.* **1990**, *268*, 101.
(39) Zhou, Z.; Chu, B. *J. Colloid Interface Sci.* **1988**, *126*, 171.
(40) Lopes, J. R.; Loh, W. *Langmuir* **1998**, *14*, 750.
(41) Yu, G. E.; Deng, Y.; Dalton, S.; Wang, Q. G.; Attwood, D.; Price, C.; Booth, C. *J. Chem. Soc., Faraday Trans.* **1992**, *88*, 2537.

JP809685Q